

## STATUS AND PERSPECTIVES OF SPIN PHYSICS\*

UTA STÖSSLEIN

Nuclear Physics Laboratory, University of Colorado at Boulder  
Campus Box 390, Boulder, CO 80309-0390, USA

and

DESY, Notkestrasse 85, 22607 Hamburg, Germany  
e-mail: [uta.stoesslein@desy.de](mailto:uta.stoesslein@desy.de)

*(Received September 16, 2002)*

The status of our understanding the spin-flavor structure of the nucleon is discussed based on most recent data from inelastic scattering experiments at SLAC, JLAB and DESY. Recent insights from current measurements and promising directions for future measurements are highlighted.

PACS numbers: 12.38.Qk, 13.60.-r, 13.60.Hb, 13.88.+e

## 1. Introduction

One of the most interesting ongoing experimental and theoretical studies involves the origin of the nucleon spin. Simple models which could rather successfully describe the hadronic spin of nuclei as the sum of spin contributions from its constituents, failed for composite objects like protons [1]. As viewed from Quantum Chromodynamics (QCD), the proton spin ought to be generated dynamically with contributions due to sea quarks and gluons including their orbital angular momenta.

The aim of this talk is to summarize most recent results in polarized electron-nucleon high-energy scattering. This includes new results on the spin structure functions  $g_1$  and  $g_2$  as well as new global analyses of  $g_1$  performed in perturbative QCD (pQCD) in Next-to-Leading Order (NLO). These analyses allows one to access mainly the contribution of the spin of the valence quarks ( $\Delta u_v$ ,  $\Delta d_v$ ) to the spin of the nucleon while the contribution of the gluons and of the sea quarks could so far be constrained somewhat.

---

\* Plenary presentation at the X International Workshop on Deep Inelastic Scattering (DIS2002) Cracow, Poland, 30 April-4 May, 2002.

First insight into the polarized sea is due to a complete determination of flavor separated quark polarizations,  $\Delta q/q$  with  $q = u, d, \bar{u}, \bar{d}, s + \bar{s}$ , in leading order pQCD using semi-inclusive double-spin asymmetries for charged pions and kaons in addition to the well-known inclusive double-spin asymmetries. Promising directions for future work regarding the still unknown orbital angular momentum of quarks, are opened by measurements of single-spin asymmetries in hard exclusive electroproduction of pions and real photons. Single-spin asymmetries in semi-inclusive electroproduction of pions give first indications of a non-zero transverse quark distribution  $\delta q$ .

A brief reminder of the peculiarities of *polarized* Deep-Inelastic Scattering (DIS) as well as perspectives of the ongoing and upcoming experiments are completing the talk. More detailed discussion and subjects which could not be covered here, may be found in the contributions to the spin session of this workshop.

## 2. Double-spin asymmetries and spin structure functions

Inclusive deep-inelastic scattering is one of the best-known examples of a factorizable process which thus allows one to explore the non-trivial internal structure of the proton. Over the past 30 years valuable information has been obtained on the parton momentum distributions and their helicity dependence. Convenient functions were initially introduced in the Quark-Parton-Model (QPM), for scattering on a spin-1/2 target by

$$q(x) = q^+(x) + q^-(x), \quad \Delta q(x) = q^+(x) - q^-(x). \quad (1)$$

The notations  $q^{+(-)}$  refer to parallel (anti-parallel) orientation of the quark and nucleon spins. The parton distributions determine the spin-averaged structure function  $F_1$  and the spin-dependent structure function  $g_1$  to be

$$F_1(x) = \frac{1}{2} \sum_q e_q^2 q(x), \quad g_1(x) = \frac{1}{2} \sum_q e_q^2 \Delta q(x). \quad (2)$$

Here, the sums extend over all quark and anti-quark distributions weighted by the electrical charge  $e_q$  squared. The second leading twist spin structure function,  $g_2$ , is expected to be zero in the naive QPM but as well measurable in DIS.

Traditionally, one of the basic quantities measured in polarized DIS, *i.e.* using longitudinally polarized charged lepton beams and polarized targets, are cross section asymmetries,  $A_{\parallel}$  and  $A_{\perp}$

$$A_{\parallel} = \left( \frac{1}{fP_B P_T} \right) \frac{\sigma^{\leftarrow\leftarrow} - \sigma^{\rightarrow\rightarrow}}{\sigma^{\leftarrow\leftarrow} + \sigma^{\rightarrow\rightarrow}} = D(A_1 + \eta A_2), \quad (3)$$

$$A_{\perp} = \left( \frac{1}{fP_B P_T} \right) \frac{\sigma^{\downarrow\rightarrow} - \sigma^{\uparrow\rightarrow}}{\sigma^{\downarrow\rightarrow} + \sigma^{\uparrow\rightarrow}} = d(A_2 - \zeta A_1), \quad (4)$$

which are closely related to the virtual photon asymmetries,  $A_1$  and  $A_2$ . Here,  $\sigma^{\rightarrow\rightarrow}$  ( $\sigma^{\leftarrow\leftarrow}$ ) denotes the cross section for the lepton and nucleon spins aligned parallel (anti-parallel), while  $\sigma^{\downarrow\rightarrow}$  ( $\sigma^{\uparrow\rightarrow}$ ) is the cross section for nucleons transversely polarized w.r.t. the beam spin orientation. The asymmetries  $A_1$  and  $A_2$  are kinematically reduced by the amount of the virtual photon polarization, denoted in Eqs. (3), (4) with  $D$  and  $d$ , where  $0 < D \approx y \leq 1$  ( $y$  is the inelasticity variable). The dilution arising from the experimental conditions is contained in the factor  $1/(P_B P_T f)$ . It accounts mainly for the values of beam and target polarizations, which are about 0.5 to 0.9 with systematic uncertainties at the level of 2% to 5% for modern spin experiments, see Table I. The factor  $f$  denotes the fraction of polarizable target material. For typical solid state target materials, as used at SLAC and CERN,  $f$  is small and varies from about 0.13 for butanol to 0.5 for lithium deuteride. It is about 0.55 for a  $^3\text{He}$  gas target (SLAC-E154). The Hermes experiment at DESY has an internal target with almost pure gases ( $f \approx 1$ ).

In spin asymmetry measurements spin-independent detector effects cancel, contrary to contributions from polarized and unpolarized radiative corrections. Eqs. (3) and (4) thus hold only for the one-photon exchange cross section. QED radiative corrections may introduce a further, kinematically dependent dilution. In particular, for large  $y$  ( $0.5 \lesssim y \leq 1$ ), the contribution from elastic radiative tails might get significant with ratios for the observed lepton–nucleon cross section to the one-photon cross section up to 2 to 3. Due to the kinematic correlation of those high  $y$  values with low Bjorken- $x$  values,  $x < 0.01$ , the access of this interesting kinematic range with a conventional forward spectrometer is very challenging, see *e.g.* results from SMC [7, 15] and recent data from Hermes [16].

The virtual photon asymmetries,  $A_1$  and  $A_2$ , can be written in terms of the spin-dependent structure functions,  $g_1$  and  $g_2$

$$A_1 = \frac{g_1 - \frac{4M^2 x^2}{Q^2} g_2}{F_1} \approx \frac{g_1}{F_1}, \quad A_2 = \frac{2Mx(g_1 + g_2)}{\sqrt{Q^2} F_1}, \quad (5)$$

where  $F_1 = F_2(1 + \frac{4M^2 x^2}{Q^2})/(2x(1+R))$  can be determined from measurements of  $R$ , which depends on the ratio of longitudinal to transverse virtual-photon absorption cross sections  $R = \sigma_L/\sigma_T$ , and of the well-known unpolarized

TABLE I

Main parameters of modern high-energy spin physics experiments.

Lab	Experiment	Year	Beam	$P_B$	Target	$P_T$	$f$		
SLAC	E142 [2]	92	19–26 GeV $e^-$	0.39	$^3\text{He}$	0.35	0.35		
		93	10–29 GeV $e^-$	0.85	$\text{NH}_3$	0.70	0.15		
					$\text{ND}_3$	0.25	0.24		
	E154 [4]	95	48 GeV $e^-$	0.83	$^3\text{He}$	0.38	0.55		
	E155 [5]	97	48 GeV $e^-$	0.81	$\text{NH}_3$	0.80	0.15		
					$\text{LiD}$	0.22	0.36		
E155X [6]	99	29/32 GeV $e^-$	0.83	$\text{NH}_3$	0.70	0.16			
				$\text{LiD}$	0.22	0.36			
CERN	SMC [7]	92	100 GeV $\mu^+$	0.81	D-butanol	0.40	0.19		
		93	190 GeV $\mu^+$	0.80	H-butanol	0.86	0.12		
		94/95		0.80	D-butanol	0.50	0.20		
		96		0.80	$\text{NH}_3$	0.89	0.16		
DESY	HERMES [8–10]	95	28 GeV $e^+$	0.55	$^3\text{He}$	0.46	1.0		
		96/97		0.55	H	0.88	1.0		
		98	28 GeV $e^-$	0.55	D	0.85	1.0		
		99/00	28 GeV $e^+$	0.55	D	0.85	1.0		
DESY	HERMES [11]	$\geq 02$	28 GeV $e^\pm$	0.55	H	0.85	1.0		
CERN	COMPASS [12, 13]	$\geq 02$	160 GeV $\mu^+$	0.80	$\text{NH}_3$	0.90	0.16		
					$\text{LiD}$	0.50	0.50		
BNL	RHIC [14]	$\geq 01$	200 GeV $p$	0.70	200 GeV $p$	0.70	1.0		

structure function  $F_2$ . Here,  $Q^2$  is the four-momentum transfer squared and  $M$  is the mass of the nucleon. From Eq. (5) one can deduce that using a longitudinally polarized target predominantly determines  $g_1$ , while DIS experiments using a transversely polarized target are sensitive to  $g_1 + g_2$ . The uncertainties of the  $R$  and  $F_2$  measurements enter directly the systematic accuracy of the present  $g_1$  measurements, where in particular the poor knowledge of  $R$  at  $x \lesssim 0.01$  and  $Q^2 \lesssim 1 \text{ GeV}^2$  becomes relevant.

The proton structure function  $g_1^p$  can be directly extracted from a longitudinally polarized hydrogen target, while, the neutron structure function  $g_1^n$  obtained either from a longitudinally polarized  $^2\text{H}$  or a  $^3\text{He}$  target requires additional nuclear corrections to be applied. The polarization of the  $^3\text{He}$  nucleus is mainly due to the neutron. Effects of the nuclear wave function

of the polarized  $^3\text{He}$  nucleus have yet to be corrected for by using  $g_1^p$  data to evaluate the proton contributions, *i.e.*,  $g_1^n(x, Q^2) = 1/\rho_n(g_1^{^3\text{He}} - 2\rho_p g_1^p)$ , where  $\rho_n = (0.86 \pm 0.02)$  and  $\rho_p = (-0.028 \pm 0.004)$  [17, 18]. Additional corrections due to the neutron binding energy and Fermi motion were shown to be small [19]. For the polarized deuteron, which is assumed to be a loosely bound  $p$ - $n$  system, the D-state component in the deuteron wave function ( $\omega_D = 0.05 \pm 0.01$  [20]) slightly reduces the deuteron spin structure function. Subtracting the large contribution due to the polarized proton one obtains  $g_1^n(x, Q^2) = 2g_1^d(x, Q^2)/((1 - 1.5\omega_D)) - g_1^p(x, Q^2)$ . A possible further contribution may arise from the still unknown tensor-polarized structure function  $b_1^d$ , a new leading twist function that occurs in case of scattering electrons off a spin-1 target [21]. In the QPM,  $b_1$  measures the dependence of the quark momentum distributions on the helicity of the target, *i.e.*  $b_1 = \frac{1}{2}(2q_{\uparrow}^0 - q_{\uparrow}^1 - q_{\downarrow}^1)$ . Here  $q_{\uparrow}^m$  ( $q_{\downarrow}^m$ ) is the probability to find a quark with momentum fraction  $x$  and spin up (down) in a hadron or nucleus with helicity  $m$ . In all  $g_1^d$  analysis so far  $b_1^d = 0$  is assumed, but first data to constrain  $b_1^d$  are expected from Hermes [22].

### 3. New inclusive data

The virtual photon asymmetries are bound by  $|A_2| \leq \sqrt{R(1 + A_1)}/2$  [23] and  $|A_1| \leq 1$ . Testing those model-independent positivity conditions is important for deeper understanding the relation between the nucleon spin and the spin of its constituents, in particular, in the limit  $x \rightarrow 1$ . For example, using an exact SU(6) symmetry ansatz,  $A_1^p = 5/9$  and  $A_1^n = 0$  is expected, but SU(6)-symmetry breaking effects imply  $A_1^{n,p} \rightarrow 1$ , see *e.g.* [25] for a discussion of various models. It is worthwhile to note that a precise knowledge of  $A_1$  and  $A_2$  can be used to derive a lower bound for  $R$  based on the above relation, in general case for each flavor separately. Here, recently two breakthroughs were achieved. A first precision measurement of  $A_2$  of the proton and the deuteron was performed by SLAC-E155X [6], showing that for  $x < 0.8$  the absolute value of  $A_2$  is much smaller than the  $\sqrt{R(1 + A_1)}/2$  limit. Another interesting new result has been obtained at Jefferson Lab. Using the longitudinally polarized 5.7 GeV electron beam ( $P_B \sim 0.81$ ) of CEBAF and a longitudinally polarized  $^3\text{He}$  gas target ( $P_T \sim 0.4$ ),  $A_1^n$  could be measured at  $x = 0.61$  and  $Q^2 = 4.9 \text{ GeV}^2$  and was determined to be positive for the first time, see Fig. 1, thus confirming SU(6) symmetry breaking in nature. An extension of this high-statistics measurement to the range of about  $0.1 < x < 0.8$  is planned based on an upgrade of CEBAF to 12 GeV [25].

Recent data on the spin structure functions  $xg_1(x, Q^2)$  and  $xg_2(x, Q^2)$  for the proton, deuteron and neutron are presented at their measured  $\langle Q^2 \rangle$  values in Fig. 2 including the new precise neutron data on  $g_1^n$  from the JLAB

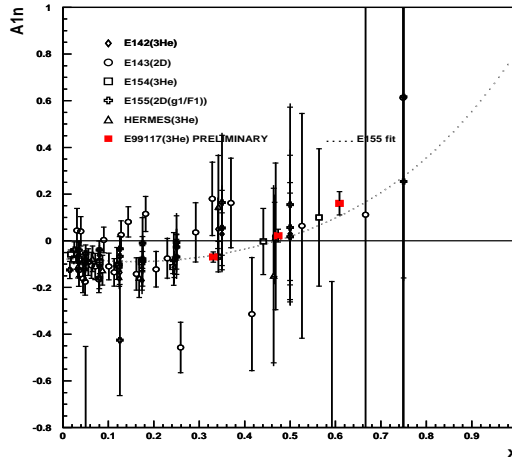


Fig. 1. Recent data on the virtual photon asymmetry  $A_1^n$  of the neutron including the new precise data from the JLAB experiment E99-117 [24] in the valence-quark region. The dashed curve is a phenomenological fit of SLAC-E155 [5].

experiment E99-117 [24]. Also shown are the final high-precision data on  $g_1^{p,d}$  from E155, and new preliminary  $g_1^{p,d}$  data from Hermes in the kinematic range  $0.002 < x < 0.85$  and  $0.1 \text{ GeV}^2 < Q^2 < 20 \text{ GeV}^2$ , where the data at small Bjorken- $x < 0.01$  belong to low photon virtualities of  $Q^2 < 1.2 \text{ GeV}^2$ . These Hermes data confirm the SMC small- $x$  and  $Q^2 > 1 \text{ GeV}^2$  data for  $A_1^{p,d}$ . Even lower  $x$  values down to  $x = 6 \times 10^{-5}$  but at extremely low  $Q^2 = 0.01 \text{ GeV}^2$  were reached by SMC with a dedicated low- $x$  trigger [15].

As seen in Fig. 2 the spin structure functions  $g_1$  and  $g_2$  are still best known for the proton, despite the recent improvements for the deuteron, and partly, for the neutron. Actually, the precision on  $g_2^{p,d}$  could be improved by a factor of three by the dedicated E155X run as compared to previous  $g_2$  data from SMC [26] and from SLAC collaborations [2,27–29]. At large  $x \sim 0.4$  the values of  $g_1$  are positive but  $g_2$  is negative, and different from zero for both the proton and the deuteron. For  $g_2$ , with so far limited accuracy, this is in contrast to the parton model expectation of  $g_2 = 0$ . There exists no simple partonic picture for  $g_2 \neq 0$  which can be understood in terms of incoherent scattering of massless, collinear partons. It turns out that  $g_2$  arises from higher-twist processes which can be described in terms of coherent parton scattering. The spin structure function  $g_2$  is thus an interesting example for a higher-twist observable representing quark-gluon correlations in the nucleon.

In fact, omitting quark mass terms,  $g_2$  can be described by a twist-two contribution, the so-called  $g_2^{\text{WW}}$  Wandzura–Wilczek-term [30] calculable from  $g_1$ , and a pure twist-3 term denoted here with  $\bar{g}_2$  reflecting the

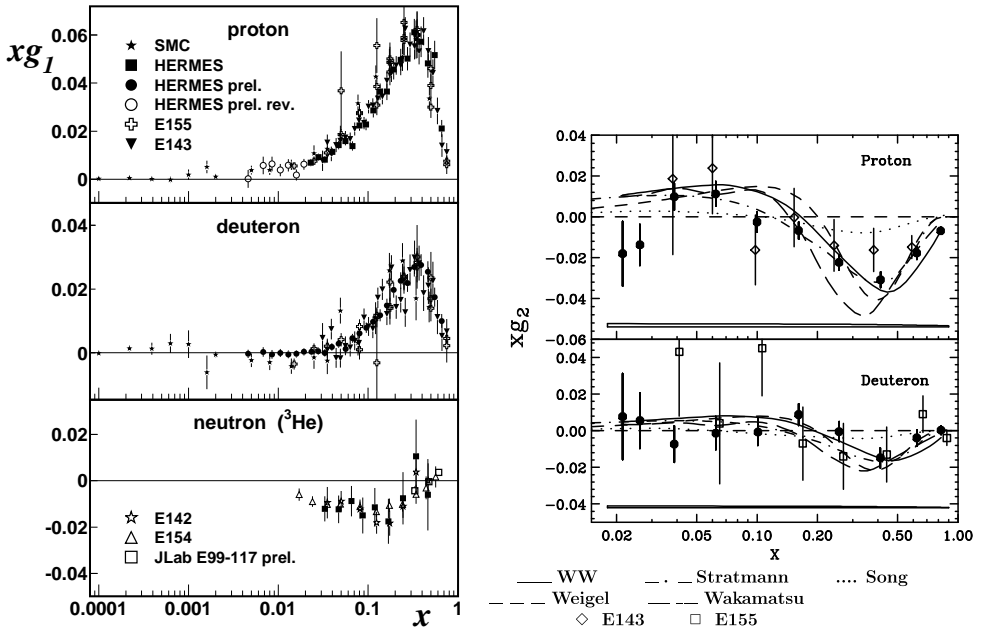


Fig. 2. Compilation of recent data on the spin structure functions  $xg_1(x, Q^2)$  (left panel) and  $xg_2(x, Q^2)$  [6] (right panel) including new data from DESY (Hermes preliminary), JLAB (E99-117 preliminary) and SLAC (E155X). All data are given at their quoted mean  $Q^2$  values. The values for  $xg_2$  are compared with the  $g_2^{\text{WW}}$  term (solid line), see text, and several bag model calculations [6].

interaction-dependent part, *i.e.*  $g_2(x, Q^2) = g_2^{\text{WW}} + \bar{g}_2(x, Q^2)$  with

$$g_2^{\text{WW}}(x, Q^2) = -g_1(x, Q^2) + \int_x^1 \frac{g_1(y, Q^2)}{y} dy. \quad (6)$$

The recent data from the  $g_2$  experiment E155X (right panel of Fig. 2) are in good agreement with the Wandzura–Wilczek approximation,  $g_2^{\text{WW}} \propto -g_1$ , which supports the observation discussed above. Consequently, any possible twist-3 term may be small. This is supported by new estimates [6] of the twist-3 matrix element  $d_2$ , obtained at an average  $Q^2$  of 5 GeV<sup>2</sup> with improved precision for the proton and the neutron, combining all SLAC  $g_2$  data,  $d_2^p = 0.0032 \pm 0.0017$  and  $d_2^n = 0.0079 \pm 0.0048$ , respectively. Here, the  $g_2^{\text{WW}}$ -term was calculated using empirical fits [5] to  $g_1$  data. Over the measured  $x$  range, the SLAC data are not in agreement with the Burkhardt–Cottingham sum rule [31], which is, however, difficult to test since it requires to measure the  $g_2$  behavior for  $x \rightarrow 0$ . The corresponding value for

the Efremov–Leader–Teryaev integral [32] is found to be  $-0.011 \pm 0.008$ , in agreement with the prediction that the valence quark contribution to the second moment of  $g_1 + 2g_2$  must be zero.

While the  $x$  dependence of the spin asymmetries and structure functions has been precisely measured and found to be strong, only little is known about their  $Q^2$  dependence. So far no evidence for a  $Q^2$  dependence of  $g_1/F_1$ , note  $g_1/F_1 \approx A_1$ , of the proton and neutron for  $Q^2 > 1 \text{ GeV}^2$  data could be detected beyond the statistical accuracy [5]. The  $Q^2$  dependence of  $A_2$  of the proton and deuteron follows approximately the behavior expected from the  $g_2^{\text{WW}}$ -term, although the statistical significance is still low [6].

Currently, at Jefferson Lab measurements of inclusive spin structure functions in the transition region from DIS to the low  $Q^2$  regime,  $Q^2 \lesssim 1 \text{ GeV}^2$ , and to the nucleon resonance region  $W \lesssim 2 \text{ GeV}$  are being performed with beam energies of 0.8–5.7 GeV. Using polarized electrons ( $P_B \sim 70\text{--}80\%$ ) scattered off polarized targets,  $g_1$  and  $g_2$  are measured in a range  $0.02 < Q^2 < 2.5 \text{ GeV}^2$ , *i.e.* complementary to the high-energy spin experiments. The preliminary results for the asymmetry  $A_1 + \eta A_2$  show significant  $Q^2$  dependencies for a  $^3\text{He}$  gas target [25] as well as for proton ( $\text{NH}_3$ ) and deuteron ( $\text{ND}_3$ ) solid state targets [33]. This behavior reflects the rapidly changing helicity structure of some resonances with the scale probed. Accurate measurements will allow stringent tests of the  $Q^2$  dependence of nucleon structure models, first moments of spin structure functions and sum rules [34] and may shed new light on the important question at which distance scale pQCD corrections will break down and physics of confinement may dominate.

#### 4. Global QCD analyses and gluon polarization $\Delta G$

In NLO pQCD, the spin structure function  $g_1$  is given by

$$g_1^{p(n)} = \frac{1}{9} \left\{ \Delta C_{\text{NS}} \otimes \left[ +(-)\frac{3}{4}\Delta q_3 + \frac{1}{4}\Delta q_8 \right] + \Delta C_S \otimes \Delta \Sigma + 2N_f \Delta C_G \otimes \Delta G \right\},$$

where  $\Delta C_{q,G}$  are the spin-dependent Wilson coefficients and  $\otimes$  denotes the convolution in  $x$  space. The usual notations for three flavours ( $N_f = 3$ ) are:

$$\begin{aligned} \Delta \Sigma &= (\Delta u + \Delta \bar{u}) + (\Delta d + \Delta \bar{d}) + (\Delta s + \Delta \bar{s}), \\ \Delta q_3 &= (\Delta u + \Delta \bar{u}) - (\Delta d + \Delta \bar{d}) = 6(g_1^p - g_1^n), \\ \Delta q_8 &= (\Delta u + \Delta \bar{u}) + (\Delta d + \Delta \bar{d}) - 2(\Delta s + \Delta \bar{s}), \\ \Delta G &\quad \text{in NLO only; } \Delta C_G^0 = 0 \text{ in LO.} \end{aligned}$$

The good description of the  $g_1$  data with  $Q^2 > 1 \text{ GeV}^2$  is illustrated for the proton case in Fig. 3 (left panel). The observed pattern of scaling violations

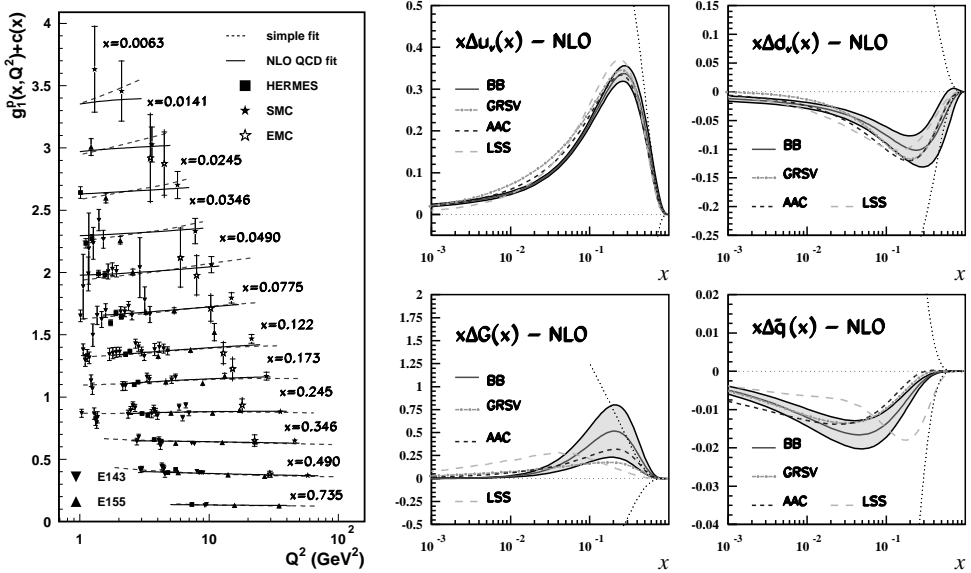


Fig. 3. Left:  $Q^2$  dependence of  $g_1^p(x, Q^2)$  for  $Q^2 > 1 \text{ GeV}^2$  data. The  $g_1^p$  values are calculated using recent data on  $g_1^p/F_1^p$  and  $F_1^p$  determined by  $F_2^p$  [35] and  $R$  [36]. To evaluate the  $Q^2$  behavior, the data has been shifted to common  $x$  values using  $F_1^p$  and  $g_1^p/F_1^p$  parameterizations. Also shown are an empirical fit according to [5] and a NLO pQCD fit [39]. Right: Polarized parton distribution functions  $x\Delta d_v$ ,  $x\Delta u_v$ ,  $x\Delta G$  and  $x\Delta\bar{q}$  from updated NLO pQCD ( $\overline{\text{MS}}$ ) fits at  $Q^2 = 4 \text{ GeV}^2$  using  $\text{SU}(3)_f$  assumptions. Labels are according to the results from [39] (BB), [41] (GRSV), [42] (AAC), and [43] (LSS). The shaded bands [39] represent the propagated statistical errors only.

of  $g_1^p$  resembles the known pattern of scaling violation in the unpolarized structure function  $F_2^p$ . Apparently, inclusive data allow linear combinations of polarized PDFs ( $\Delta q + \Delta\bar{q}$ ) and the gluon polarization  $\Delta G$ , as an  $\mathcal{O}(\alpha_s)$  correction, to be accessed by solving the DGLAP evolution equations. The mixing of the evolution of the quark singlet contribution  $\Delta\Sigma$  and  $\Delta G$  yields to renormalization and factorization scheme dependent results in NLO pQCD. Frequently used schemes are the  $\overline{\text{MS}}$ , Adler–Bardeen (AB) or JET schemes, see *e.g.* [37]. In the AB and JET schemes,  $\Delta\Sigma$  is conserved and defined to be a scale-independent quantity, which is related to the  $\overline{\text{MS}}$  result by  $\Delta\Sigma(Q^2)_{\overline{\text{MS}}} = \Delta\Sigma_{\text{AB(JET)}} - N_f\alpha_s(Q^2)/(2\pi)\Delta G(Q^2)$ . The polarized gluon distribution is the same in all schemes,  $\Delta G(Q^2)_{\overline{\text{MS}}} = \Delta G(Q^2)_{\text{AB(JET)}}$ . Observed differences of  $\Delta G$  values obtained might still point to systematic differences in the applied formalism, which include the treatment of quark masses and flavours, the value of the strong coupling constant  $\alpha_s$  and the use of non-DIS data for further constraints, for example.

Several groups have been performing spin-dependent NLO pQCD fits. The SMC collaboration was the first to carefully treat statistical, systematic and theoretical uncertainties [38] in polarized DIS. A novel attempt to propagate the statistical errors through the evolution procedure was done in [39] and is presented in Fig. 3 (right panel) together with other recent NLO fit results [37, 41, 42]. Predominantly due to the inclusive proton data the positive up-valence quark polarization are now determined with good precision. Present neutron and deuteron data constrain well the negative down-valence quark polarization, but further improvements are expected including the new Hermes  $g_1^d$  data in these global fits. The polarized sea is determined to be negative while  $\Delta G$  is suggested to be positive. However, both distributions have large uncertainties as illustrated with the bands in Fig. 3 (right panel).

Spin-dependent pQCD analyses begin to become sensitive to the value of  $\alpha_s$  as well. A recent determination of  $\alpha_s$  yields  $\alpha_s(M_Z^2) = 0.114 \pm 0.005(\text{stat})^{+0.010}_{-0.009}(\text{scales})$  [39] which is consistent with the value of the current world average  $\alpha_s(M_Z^2) = 0.118 \pm 0.002$  [40].

Present pQCD analyses use information from neutron and hyperon  $\beta$ -decays to constrain the first moments of the non-singlet distributions,  $a_3 = \Delta q_3 = F + D = 1.267 \pm 0.0035$  and  $a_8 = \Delta q_8 = 3F - D = 0.585 \pm 0.025$ . Assuming  $SU(3)_f$  flavour symmetry the first moment of  $g_1$  is given by

$$\Gamma_1(Q^2) = C_S(Q^2)a_0(Q^2) + C_{NS}(Q^2)\frac{1}{12}\left(\left|\frac{g_a}{g_v}\right| - \frac{1}{3}(3F - D)\right), \quad (7)$$

where  $|g_a/g_v|$  is the axial coupling constant and  $a_0(Q^2)$  is the axial charge. An update of the E154 [44] NLO pQCD fit in the  $\overline{MS}$  scheme was performed by the E155 collaboration [5] using published data. It confirms the quark singlet contribution  $\Delta\Sigma$  to be small,  $\Delta\Sigma = 0.23 \pm 0.04(\text{stat}) \pm 0.06(\text{syst})$  at  $Q^2 = 5 \text{ GeV}^2$ , well below the prediction of 0.58 [45]. The value for  $\Gamma_1^p - \Gamma_1^n = 0.176 \pm 0.003 \pm 0.007$  is found to be in agreement with the Bjorken sum rule prediction of  $0.182 \pm 0.005$ . For the first moment of the gluon distribution a value of  $\Delta G = 1.6 \pm 0.8(\text{stat}) \pm 1.1(\text{syst})$  is obtained. Apparently, the uncertainty on  $\Delta G$  from scaling violations is still too large to significantly constrain the gluon contribution to the nucleon spin. The value of  $a_8$  depends on the assumption of  $SU(3)_f$  flavour symmetry among hyperons, which is known to be inexact. Indications of a breakdown of  $SU(3)$  flavor symmetry, as observed in the hyperon  $\beta$  decay, and its impact on the polarized PDFs were discussed recently [46]. While the influence on the singlet and non-strange quark polarizations was found to be small, the strange sea quark and gluon polarizations change significantly when  $SU(3)_f$  symmetry breaking effects are considered [46]: *e.g.*  $\Delta s + \Delta\bar{s}$  varies from  $-0.02$  to  $-0.15$  and  $\Delta G$  from 0.13 to 0.84. The observed strong dependence of the gluon and

strange quark polarizations on the  $SU(3)_f$  symmetry assumptions calls for more direct probes for a determination of those quantities. A first attempt to determine  $\Delta G/G$  in LO pQCD from the photon–gluon fusion process was presented by Hermes [47]. Using PYTHIA [48], the gluon polarization has been found to be positive,  $\langle \Delta G/G \rangle = 0.41 \pm 0.18$  (stat)  $\pm 0.03$  (syst), at  $\langle p_T^2 \rangle = 2.1 \text{ GeV}^2$  and  $\langle x_G \rangle = 0.17$ . A similar  $\Delta G/G$  analysis is being performed by Hermes based on the high statistics deuteron data of the run periods 1998–2000 [49] and is being expected from COMPASS [50]. The interpretation of such data is still limited to LO pQCD, since NLO simulation programs are not available yet.

### 5. Flavor separation of polarized quark distributions

Information on the flavor separated polarized valence and sea quark contributions can possibly be obtained via semi-inclusive scattering, where one or more hadrons  $h$  in coincidence with the scattered charged lepton are detected. According to the favored fragmentation process, the charge of the hadron and its quark composition provide sensitivity to the flavor of the struck quark as is transparent within the QPM. Assuming the hard scattering and the fragmentation process to factorize, the double-spin asymmetries for hadrons,  $A_1^h$ , can be separated into  $z$  and  $x$  dependent terms,

$$A_1^h(x, Q^2) \approx \frac{g_1^h}{F_1^h}(x, Q^2) = \frac{\int_{z_{\min}}^{z_{\max}} dz \sum_q e_q^2 \Delta q(x, Q^2) D_q^h(z, Q^2)}{\int_{z_{\min}}^{z_{\max}} dz \sum_q e_q^2 q(x, Q^2) D_q^h(z, Q^2)}. \quad (8)$$

The fragmentation function  $D_q^h(z, Q^2)$  is the probability that the hadron  $h$  with energy  $E_h$  originates from the struck quark flavor  $q$ , a process which is assumed to be spin-independent. The hadron momentum fraction in the lab frame is given by  $z = E_h/\nu$ , where  $\nu$  is the energy of the virtual photon.

Measurements of semi-inclusive hadron asymmetries had been performed by EMC [1], SMC [51] and Hermes [52], but were restricted to a three-flavor separation so far. Here, most recent results from Hermes [53] on a five-flavor separation of the quark polarizations  $\Delta u/u$ ,  $\Delta d/d$ ,  $\Delta \bar{u}/\bar{u}$ ,  $\Delta \bar{d}/\bar{d}$ ,  $(\Delta s + \Delta \bar{s})/(s + \bar{s})$  will be discussed.

New Hermes results on  $A_1^h$  are shown in Fig. 4. They are based on the full high statistics set of deuterium data of the years 1998–2000, employing for a momentum range of 2 to 15 GeV the pion and kaon identification capability of a dual-radiator Ring Imaging Čerenkov detector. To maximize the sensitivity to the struck current quark, typically kinematic cuts of  $W^2 > 10 \text{ GeV}^2$ ,  $z > 0.2$  and  $x_F > 0.1$  are imposed on the data in order to suppress

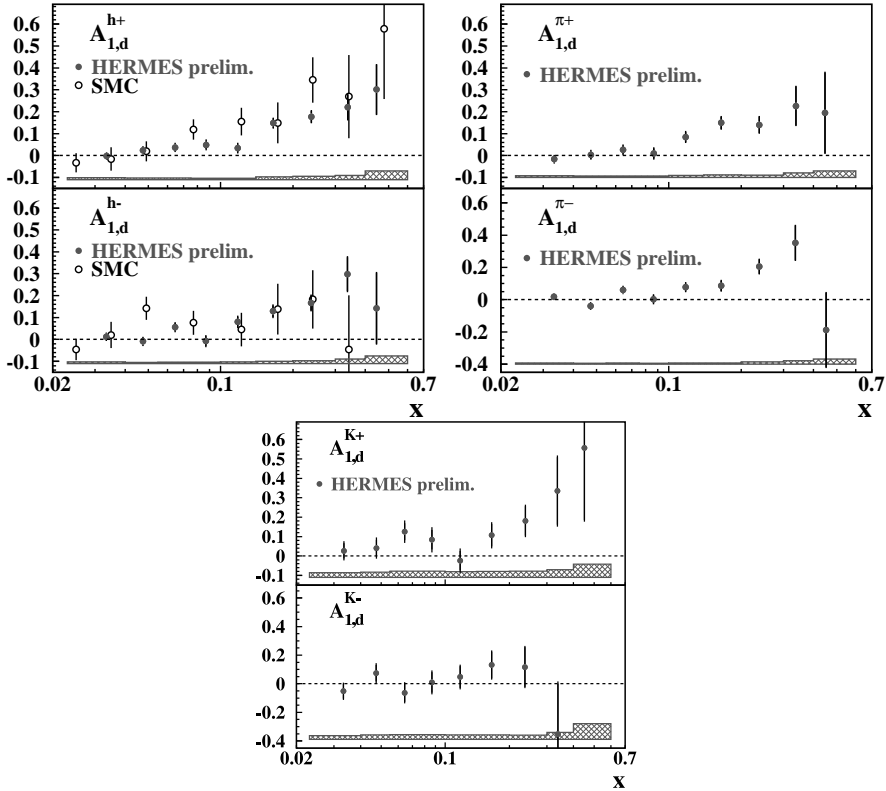


Fig. 4. Semi-inclusive asymmetries for positively and negatively charged hadrons (top left), pions (top right) and kaons (bottom) from Hermes [53] (preliminary) with systematic uncertainties (bands). Previous data from SMC [51] are also shown.

effects from target fragmentation, while the use of  $z_{\max} = 0.8$  suppresses possible contributions from the exclusive production of  $\rho^0$  mesons [54].

According to Eq. (8), the semi-inclusive asymmetries are sensitive to the quark polarizations weighted with unpolarized fragmentation functions. Following the Hermes analysis [52], a *flavor tagging* probability may be determined by simulation using the LUND string fragmentation model [55], tuned to hadron multiplicities as measured at Hermes. This allows in LO pQCD the polarized quark distributions to be extracted, see Fig. 5 (left panel), using the measured inclusive and semi-inclusive asymmetries from the proton and deuterium targets. The present asymmetry set is still most sensitive to the light valence quark polarizations ( $\Delta u_v$ ,  $\Delta d_v$ ) because of  $u(d)$ -quark dominance: the production of  $h^\pm$  is dominated by scattering off  $u(d)$  quarks from a proton(neutron) target. However, for example, the spin asymmetry of  $K^-$ , a true sea object, will have higher sensitivity to the polarization of

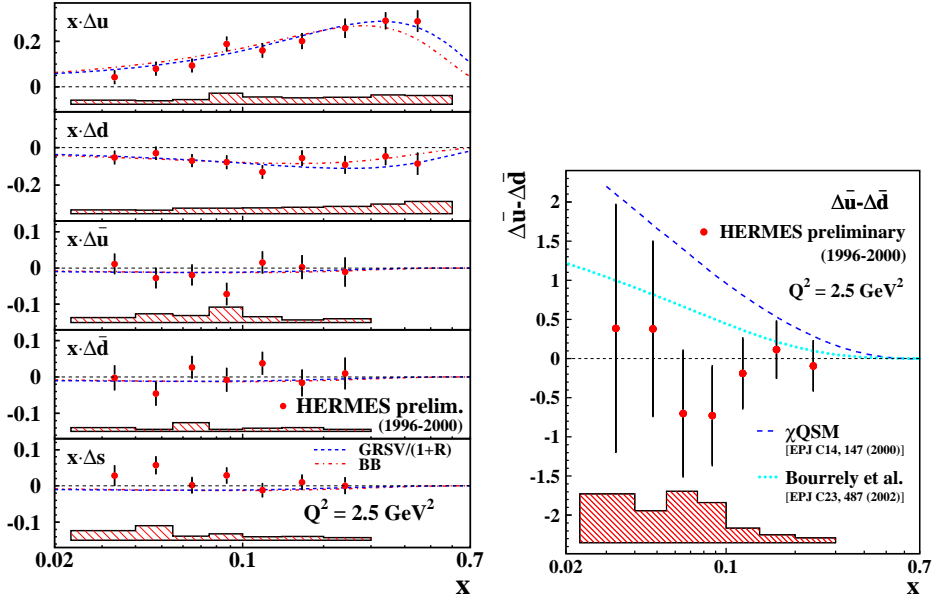


Fig. 5. Left: New Hermes results on polarized quark distributions  $x\Delta q(x)$  from inclusive and semi-inclusive asymmetries on proton and deuteron targets [53]. Data are evolved to a common  $Q^2 = 2.5 \text{ GeV}^2$  and compared with results from global LO pQCD fits from [41] (dashed) and [39] (dotted). Right: Flavor symmetry of the light polarized sea,  $\Delta \bar{u}(x) - \Delta \bar{d}(x)$ , at  $Q^2 = 2.5 \text{ GeV}^2$ . The data are compared with two recent models. Hermes systematic uncertainties are presented as bands.

the quark sea. In particular, the sensitivity of the various semi-inclusive asymmetries to the sea polarizations at  $0.02 < x < 0.2$  depending on the target, hadron type and charge can be estimated as

- $A_1(h^+)$  from  $p, n$ :  $\Delta \bar{u}$  and  $\Delta \bar{d} \sim 5 \dots 10\%$
- $A_1(h^-)$  from  $p(n)$ :  $\Delta \bar{u}$  ( $\Delta \bar{d}$ )  $\sim 10 \dots 30\%$
- $A_1(K^+)$  from  $p, n$ :  $\Delta \bar{s} \lesssim 10\%$
- $A_1(K^-)$  from  $p, n$ :  $\Delta s \lesssim 10\%$ .

The numbers illustrate the impact of the new Hermes deuterium data which allow for the first time the polarized sea quark distributions to be extracted. Fig. 5 (left panel) represents as well as Fig. 3 (right panel) the first moments at fixed  $Q^2$  which determine the flavor separated quark contributions to the proton spin: a positive (parallel to the proton spin) up quark and a negative (anti-parallel to the proton spin) down quark polarization are found. The light polarized sea quark distributions are consistent with zero, while the result for the strange quarks favors slightly positive values at small  $x < 0.1$ .

Within the present level of experimental uncertainties, the results are still in agreement with spin-dependent global LO pQCD fits where the flavor undifferentiated polarized sea is found to be small but negative.

As is seen in the right panel of Fig. 5, no significant breaking of the flavor symmetry of the polarized light sea could be observed. This is in contrast to expectations arising from models which can explain, in agreement with the Gottfried sum rule data, the flavor asymmetry of the unpolarized light anti-quark distributions in the proton,  $\bar{d}(x) - \bar{u}(x) > 0$ . A violation of the flavor symmetry has been expected to be stronger in the polarized case than in the unpolarized case, with the prediction that in the proton  $\Delta\bar{u} > 0 > \Delta\bar{s} > \Delta\bar{d}$  and  $\Delta\bar{u} - \Delta\bar{d} > \bar{d} - \bar{u} > 0$  [57]. Predictions are coming *e.g.* from the chiral quark soliton model [56], statistical models for polarized and unpolarized structure functions and PDFs [57,58], pQCD analyses with flavor-asymmetric light sea densities implementing Pauli-blocking by the valence quark [41], or an effect of the pion cloud of the nucleon [59]. To go beyond the Hermes result requires more sensitive tests for  $\Delta\bar{u}(x)$  and  $\Delta\bar{d}(x)$ . Promising are here measurements of the various helicity asymmetries for  $W^\pm$  production in polarized pp collisions at high energies, which will be measured with experiments at RHIC-BNL, see *e.g.* [60] and [57,58].

## 6. Exclusive spin physics

In hard exclusive processes as leptonproduction of either a real photon (DVCS) or a meson, new hadronic parton distributions appear which contain information on the origin of nucleon spin that DIS can not provide and which may allow to probe the longitudinal and transverse structure of the nucleon in a correlated manner [61]. Based on impressive theoretical efforts in the last decade, a QCD description of such reactions could be achieved, separating the soft physics inherent to this process from the hard one by extending the framework of DIS to the off-forward region of the virtual Compton process, for a recent review see *e.g.* [62]. The non-perturbative functions are the so-called generalized parton distribution functions. GPDs (usually denoted with  $H, E, \tilde{H}, \tilde{E}$ ) represent probability amplitudes to knock out a parton from a nucleon and to put it back with different longitudinal momentum fractions parametrized by  $\xi$  (skewness parameter) and  $x$ . GPDs depend also on the Mandelstam invariant  $t$ , the squared momentum transfer to the nucleon. These complex functions of multiple variables unify known concepts of hadronic physics, *e.g.* by linking ordinary parton distribution functions and nucleon form factors.

In the context of spin physics, the attractive fact is that the total angular momentum  $J_q$  and  $J_G$  carried by a quark flavor and by a gluon, respectively, are given by the second moment of the sum of their unpolarized GPDs

$(H^q, E^q)$  in the limit  $t = 0$  [63]. The total angular momenta of partons are still unknown and related by angular momentum conservation to the spin of the nucleon projected along an axis. The latter could be written also as a sum of contributions from quark ( $\Delta\Sigma$ ) and gluon ( $\Delta G$ ) spin and orbital angular momentum of quarks ( $L_q$ ) and of gluons ( $L_g$ ) [63, 64]

$$\frac{1}{2} = J_q + J_g = \frac{1}{2}\Delta\Sigma + L_q + \Delta G + L_g. \quad (9)$$

To understand the composition of the nucleon spin finally, each contribution has to be identified. The usefulness of such angular momentum sum rule in the sense of a gauge invariant definition and measurability of each of the terms are yet under discussion [65], especially with respect to the gluon.

The DVCS channel is viewed to be a particular clean hadronic reaction that gives access to the GPDs [66]. In the case of hard lepton production of mesons, however, the theoretical description involves with the meson distribution amplitudes another unknown non-perturbative input, which may complicate the identification of the GPDs. So far, the experimental data and GPD models focus on the proton but GPDs for the deuteron were also introduced recently.

First experimental results on lepton beam helicity dependent asymmetries associated with DVCS were obtained from Hermes [68] and confirmed by the CLAS collaboration [69], see Fig. 6 (left panel). This single-spin asymmetry is sensitive to the interference term formed from the imaginary part of the DVCS amplitudes, which can be expressed in terms of GPDs, and the background Bethe–Heitler amplitude. In a LO leading twist description, this leads to a  $\sin\phi$  dependence in the related asymmetry,  $A(\phi) = \alpha \text{sign}(e) \sin\phi$ . Here,  $\text{sign}(e)$  represents the sign of the beam charge and  $\phi$  is the angle between the  $\gamma$  and  $e$  scattering planes. The integrated beam-spin asymmetry obtained from positron scattering off a hydrogen target at Hermes is  $\alpha = -0.23 \pm 0.04(\text{stat}) \pm 0.03(\text{syst})$ , while electron scattering at CLAS yields  $\alpha = 0.202 \pm 0.021(\text{stat}) \pm 0.009(\text{syst})$ . Both results are in fair agreement with a simple  $\sin\phi$  dependence, and a change in the sign is seen with the beam charge used. More precise data are expected to become available from both experiments allowing the significance of higher  $\sin\phi$  moments to be tested which are sensitive to quark–gluon correlations as described by twist-three GPDs.

In the right panel of Fig. 6, first results from Hermes [70] on a beam-charge asymmetry associated with DVCS are presented. This measurement combines data from electron and positron scattering off unpolarized targets. The single-spin asymmetry is sensitive to the interference term related with the real part of the DVCS amplitudes, and is expected to follow a  $\cos\phi$  dependence. A corresponding fit to the data reveals a positive amplitude of  $0.11 \pm 0.04(\text{stat}) \pm 0.03(\text{syst})$ .

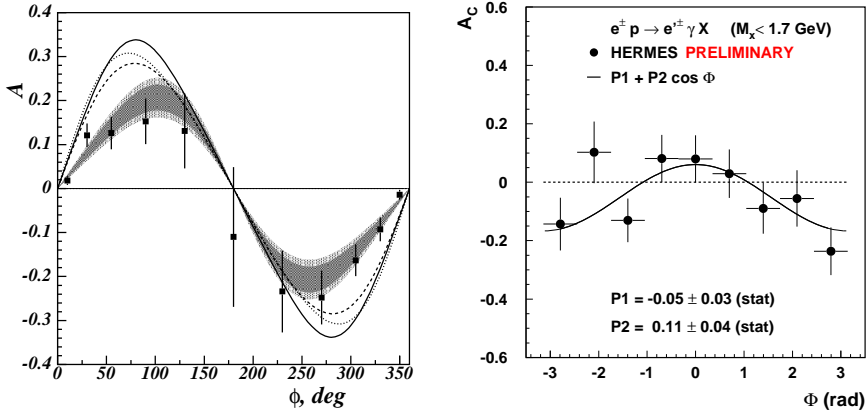


Fig. 6. Left: Beam-spin asymmetry associated with DVCS as a function of  $\phi$  from the CLAS [69] experiment [69]. The curves are from model calculations. The shaded area (right) represents the uncertainties of the best phenomenological  $\phi$  dependent fit functions. Right: Beam-charge asymmetry associated with DVCS as a function of  $\phi$  from Hermes [70]. The data correspond to a missing mass region between  $-1.5$  GeV and  $+1.7$  GeV. The solid line is a  $\cos \phi$  fit to the data.

Since only a quadratic combination of GPDs appears in the unpolarized DVCS cross section [71], the use of polarization might help to access additional observables which have different sensitivities to the various GPDs. For example, it has been predicted [72] that for the exclusive production of  $\pi^+$  mesons from a transversely polarized target by longitudinally virtual photons, the interference between the pseudoscalar ( $\tilde{E}$ ) and pseudovector ( $\tilde{H}$  with  $\tilde{H} \rightarrow \Delta q$  in forward limit at  $t = 0$ ) amplitudes leads to a large asymmetry in the distribution of  $\phi$ , the azimuth of the pion around the lepton scattering plane.

Recently Hermes presented first data on single-spin azimuthal asymmetries measured in the reaction  $ep \rightarrow e'\pi X$  using *longitudinally* polarized protons [73, 74], see Fig. 7. Comparing the left and right panels of Fig. 7 it is clearly seen, that for  $\pi^+$  production at high  $z$  ( $> 0.9$ ) the  $\sin \phi$  moment of the asymmetry is observed [73] to become suddenly negative, in agreement with a different (but related) analysis of exclusive  $\pi^+$  data [74]. A fit to the exclusive data,  $A(\phi) = A_{UL}^{\sin \phi} \sin \phi$ , delivers the  $\sin \phi$  moment of the target-spin related asymmetry to be  $A_{UL}^{\sin \phi} = -0.18 \pm 0.05$  (stat)  $\pm 0.02$  (syst) integrated over the kinematic range. However, for a complete quantitative modelling of the observed asymmetry the upcoming Hermes and COMPASS data on transversely polarized targets are required.

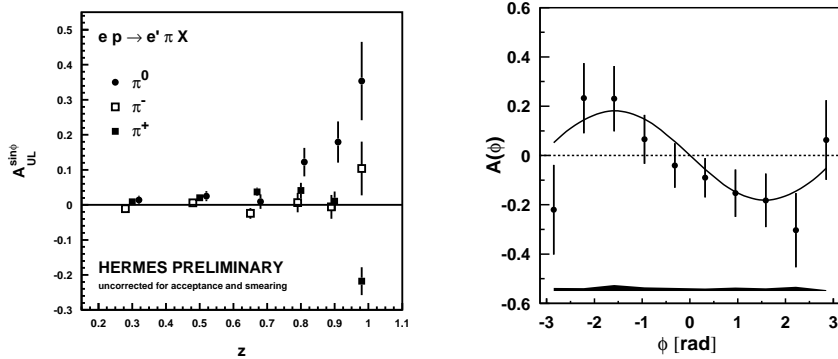


Fig. 7. Hermes results on azimuthal  $\sin \phi$  moments of the single-spin asymmetries measured for the production of charged and neutral pions, as a function of the pion momentum fraction  $z$  [73] (left) and for the exclusive  $\pi^+$  production [74] (right). Exclusive  $\pi^+$  was selected by requiring the missing mass  $M_X$  of the reaction  $e^+p \rightarrow e^+\pi^+X$  corresponded to the nucleon mass,  $M_X < 1.05$  GeV. The curve is a fit to the data by  $A(\phi) = A_{UL}^{\sin \phi} \sin \phi$ . The subscripts U and L indicate the use of an unpolarized beam and a longitudinally polarized target, respectively.

Regarding new experiments one of the most interesting questions is to determine the still unknown third type of twist-two quark distribution function  $\delta q$ , called transversity, introduced in [75]. In order to probe the transverse spin polarization of the nucleon, a helicity (identical to chirality at leading twist) flip of the struck quark must have occurred. In hard processes this is only possible with non-zero quark masses, thus suppressing this function in inclusive DIS. However, in semi-inclusive processes it is possible to combine two chiral odd parts, one describing the quark content of the target ( $\delta q$ ) and another one describing the quark fragmentation into hadrons. Considerable effort has gone into understanding, modelling and into possible measures of  $\delta q$ , for a review see [76].

There are important differences to be noted between the helicity and the transversity distributions which give further insight into the non-perturbative QCD regime of hadronic physics. For example, as mentioned before, quark and gluon helicities mix under  $Q^2$  evolution, but there is no analogue of gluon transversity in the nucleon. Furthermore, the difference between  $\Delta q$  and  $\delta q$  reflects the relativistic character of quark motion in the nucleon. Only in the case of non-relativistic movements of quarks in the nucleon  $\Delta q$  and  $\delta q$  become identical, *i.e.* invariant under a series of boosts and rotations which convert the longitudinally polarized nucleon into a transversely polarized one. The first moments of the transversity distributions for quarks and anti-quarks are related to the flavor dependent contribution to the nucleon tensor charge  $\delta \Sigma$ . This is expected to be a more non-singlet like quantity in contrast to the axial charge, but more difficult to predict [77].

The recent observation by the Hermes collaboration [78, 79] of non-zero single-spin azimuthal asymmetries for neutral and positively charged pions off a proton target generated much interest, since it can be interpreted as evidence for a non-zero chirality-flipping fragmentation function that couples to the quark transversity distributions. The observation is further confirmed by new results on single-spin asymmetries of pions and kaons from a deuterium target, see these proceedings. However, the Hermes data were taken with longitudinally polarized targets which complicates the interpretation of the asymmetries due to possible additional twist-three contributions [80].

Transversity is an important part of ongoing and forthcoming experiments [88] and has been discussed also within this workshop series [81]. At BNL-RHIC interesting processes involving transversity in  $pp$  collisions are Drell-Yan lepton pair production with two protons transversely polarized or alternatively, chiral-odd two-pion interference fragmentation in large  $p_T$  pion pair production using one proton transversely polarized. The study of transversity distributions and chiral-odd fragmentation functions, at least for the up-quark with good precision, is a primary goal of the Hermes Run II [11, 80] using a transversely polarized hydrogen target. The COMPASS [50] experiment at CERN has a transversity programme similar to that of Hermes covering a different kinematic region. Currently, data are being taken by both experiments.

The primary goal of the COMPASS muon programme is the measurement of the gluon polarization  $\Delta G/G$  with  $\sim 0.1$  accuracy via open charm production and hadron pair production at large  $p_T$  for  $0.04 x_G < 0.3$  about. At RHIC, prompt photon production will be employed to measure the helicity-dependent gluon density  $\Delta G$ , at  $0.02 < x_G < 0.3$  [82]. A compilation of simulated statistical accuracies for  $\Delta G/G$  may be found *e.g.* in [83]. It is important that various channels for extracting  $\Delta G$  in  $eN$ - and  $pp$ -scattering are employed to minimize the (so far strong) model-dependencies.

## 7. Conclusion

Spin physics remains an exciting, rapidly developing field of research and contributes remarkably to the QCD picture of the structure of the nucleon. Recent precise spin structure function data from DESY and SLAC, together with previous data, improve the knowledge about the contribution of valence quarks to the nucleon spin within the framework of NLO pQCD and allow the fundamental Bjorken sum rule to be tested. New semi-inclusive double-spin asymmetry data from Hermes deliver additional sensitivity required for a complete flavor separation of polarized parton distributions, so far in LO pQCD. Within the present accuracy of the data, no significant breaking of the flavor symmetry of the polarized light sea could be observed. The

contribution of gluons to the nucleon spin is not yet well known. It is suggested to be positive from LO/NLO pQCD fits based on inclusive DIS data and from a LO pQCD interpretation of Hermes high  $p_T$  hadron pair production data.

A recent interesting development in QCD spin physics was triggered by the Hermes measurement of single-spin azimuthal asymmetries in semi-inclusive pion electroproduction off a longitudinally polarized target. This observation suggests a non-zero chiral-odd fragmentation function which allows the so far unknown quark transversity distribution in semi-inclusive scattering off transversely polarized targets to be accessed. For the first time, a window may be opened to access angular momenta of partons using the framework of generalized parton distribution functions based on new data on spin-dependent, hard exclusive processes, released by the Hermes and CLAS collaborations. Further experimental studies of the connection of semi-inclusive with exclusive reactions, and of high energy with low energy spin physics are being performed at JLAB and at DESY.

More precise data are expected to soon become available on the gluon spin, on flavor separated quark and anti-quark helicities and on transversity properties from the high luminosity experiments at CERN, DESY, JLAB and RHIC-Spin, and also from an upcoming SLAC experiment [84]. The perspectives also of future polarized lepton-nucleon fixed-target [83,85] and collider [86] experiments are being discussed intensively. The goal remains to develop a complete, firm theoretically picture of the momentum and spin structure of nucleons and hadrons.

I would like to thank the organizers, in particular Jan Kwieciński, for hosting such a fruitful workshop.

## REFERENCES

- [1] European Muon Collaboration, J. Ashman *et al.*, *Phys. Lett.* **B206**, 364 (1988); J. Ashman *et al.*, *Nucl. Phys.* **B328**, 1 (1989).
- [2] E142 Collaboration, P.L. Anthony *et al.*, *Phys. Rev.* **D54**, 6620 (1996).
- [3] E143 collaboration, K. Abe *et al.*, *Phys. Rev.* **D58**, 112003 (1998).
- [4] E154 Collaboration, K. Abe *et al.*, *Phys. Rev. Lett.* **79**, 26 (1997).
- [5] E155 Collaboration, P.L. Anthony *et al.*, *Phys. Lett.* **B493**, 19 (2000).
- [6] E155X Collaboration, P.L. Anthony *et al.*, arXiv:hep-ex/0204028.
- [7] Spin Muon Collaboration, B. Adeva *et al.*, *Phys. Rev.* **D58**, 112001 (1998).
- [8] HERMES Collaboration, K. Ackerstaff *et al.*, *Phys. Lett.* **B404**, 383 (1997).
- [9] HERMES Collaboration, A. Airapetian *et al.*, *Phys. Lett.* **B442**, 484 (1998).

- [10] P. Lenisa for the Hermes Collaboration, see in [87].
- [11] M.G. Vincter for the Hermes Collaboration, see in [88].
- [12] COMPASS, A Proposal for a COmmon Muon and Proton Apparatus for Structure and Spectroscopy, CERN/SPSLC 96-14, SPSLC/P27, 1 March 1996.
- [13] E.M. Kabuss for the COMPASS Collaboration, see in [89].
- [14] Polarized Proton Collider at RHIC, <http://www.agsrhichome.bnl.gov/RHIC/Spin>.
- [15] Spin Muon Collaboration, B. Adeva *et al.*, *Phys. Rev.* **D60**, 072004 (1999).
- [16] L. DeNardo for the Hermes Collaboration, to appear in Proceedings of Advanced Study Institute - Symmetries and Spin, PRAHA-SPIN-2001, Prague, Czech Republic, July 15–28, 2001.
- [17] J.L. Friar *et al.*, *Phys. Rev.* **C42**, 2310 (1990).
- [18] C. Ciofi degli Atti *et al.*, *Phys. Rev.* **C48**, 968 (1993).
- [19] R. Blankleider, R.M. Woloshyn, *Phys. Rev.* **C29**, 538 (1984); R.W. Schulze, P.U. Sauer, *Phys. Rev.* **C48**, 38 (1993).
- [20] M. Lacombe *et al.*, *Phys. Lett.* **B101**, 139 (1981).
- [21] P. Hoodbhoy, R.L. Jaffe, A. Manohar, *Nucl. Phys.* **B312**, 571 (1989); K. Bora, R.L. Jaffe, arXiv: hep-ph/9711323.
- [22] U. Stösslein for the Hermes Collaboration, see in [87]; M. Contalbrigo for the Hermes Collaboration, to appear in Proceedings of 15th International Spin Physics Symposium (SPIN2002), Brookhaven National Lab., NY, USA, Sept. 9–14, 2002.
- [23] J. Soffer, O.V. Teryaev, *Phys. Lett.* **B490**, 106 (2000).
- [24] JLab E99-117, spokespersons: J.P. Chen, Z.E. Meiziani, P. Souder.
- [25] Z.-E. Meiziani, *Nucl. Phys.* **B105**, 105 (2002).
- [26] Spin Muon Collaboration, D. Adams *et al.*, *Phys. Lett.* **B336**, 125 (1994).
- [27] E143 Collaboration, K. Abe *et al.*, *Phys. Rev. Lett.* **76**, 587 (1996).
- [28] E154 Collaboration, K. Abe *et al.*, *Phys. Lett.* **B404**, 377 (1997).
- [29] E155 Collaboration, P.L. Anthony *et al.*, *Phys. Lett.* **B458**, 530 (1999).
- [30] W. Wandzura, F. Wilczek, *Phys. Lett.* **B172**, 195 (1977).
- [31] H. Burkhardt, W.N. Cottingham, *Ann. Phys.* **56**, 453 (1970).
- [32] A.V. Efremov, O. V. Teryaev, E. Leader, *Phys. Rev.* **D55**, 4307 (1997).
- [33] G. Dodge for the CLAS Collaboration, to appear in [90].
- [34] V.D. Burkert, *Nucl. Phys.* **A699**, 261 (2002).
- [35] H. Abramowicz, A. Levy, arXiv:hep-ph/9712415.
- [36] L.W. Withlow *et al.*, *Phys. Lett.* **B250**, 193 (1990).
- [37] E. Leader, A.V. Sidorov, D. Stamenov, *Phys. Lett.* **B445**, 232 (1998).
- [38] Spin Muon Collaboration, B. Adeva *et al.*, *Phys. Rev.* **D58**, 112002 (1998).
- [39] J. Blümlein, H. Böttcher, *Nucl. Phys.* **B636**, 225 (2002).
- [40] Particle Data Group, *Eur. Phys. J.* **C15**, 91 (2000).

- [41] M. Glück *et al.*, *Phys. Rev.* **D63**, 094005 (2001).
- [42] Asymmetry Analysis Collaboration, Y. Goto *et al.*, *Phys. Rev.* **D62**, 034017 (2000).
- [43] E. Leader, A.V. Sidorov, D.B. Stamenov, *Eur. Phys. J.* **C23**, 479 (2002).
- [44] E154 Collaboration, K. Abe *et al.*, *Phys. Lett.* **B405**, 180 (1997).
- [45] J. Ellis, R. Jaffe, *Phys. Rev.* **D9**, 1444 (1974); *Phys. Rev.* **D10**, 1669 (1974) (E.).
- [46] E. Leader, A.V. Sidorov, D. Stamenov, arXiv:hep-ph/0106214.
- [47] Hermes Collaboration, A. Airapetian *et al.*, *Phys. Rev. Lett.* **84**, 2584 (2000).
- [48] T. Sjöstrand, *Comput. Phys. Commun.* **82**, 74 (1994); PYTHIA ver. 5.724.
- [49] E.C. Aschenauer for the Hermes Collaboration, to appear in [90].
- [50] F.-H. Heinsius for the COMPASS Collaboration, to appear in [90].
- [51] B. Adeva *et al.*, Spin Muon Collaboration, *Phys. Lett.* **B420**, 180 (1998).
- [52] Hermes Collaboration, K. Ackerstaff *et al.*, *Phys. Lett.* **B464**, 123 (1999).
- [53] M. Beckmann for the Hermes Collaboration, to appear in Proceedings of Workshop on Testing QCD through Spin Observables in Nuclear Targets, University of Virginia, Charlottesville, Virginia, USA, April 18–20, 2002.
- [54] V. Uleshchenko, A. Szczurek, *Acta Phys. Pol.* **B33**, 3299 (2002).
- [55] G. Ingelman, A. Edin, J. Rathsman, DESY Report 96-057 (1996).
- [56] B. Dressler, K. Goeke, V. Polyakov, C. Weiss, *Eur. Phys. J.* **C14**, 147 (2000).
- [57] R.S. Bhalerao, *Phys. Rev.* **C63**, 025208 (2001).
- [58] C. Bourrely, J. Soffer, F. Buccella, *Eur. Phys. J.* **C23**, 487 (2002).
- [59] R.J. Fries, A. Schafer, C. Weiss, arXiv:hep-ph/0204060 and references therein.
- [60] G. Bunce, N. Saito, J. Soffer, W. Vogelsang, *Ann. Rev. Nucl. Part. Sci.* **50**, 525 (2000).
- [61] M. Diehl, arXiv:hep-ph/021119.
- [62] K. Goeke, M.V. Polyakov, M. Vanderhagen, *Prog. Part. Nucl. Phys.* **47**, 401 (2001).
- [63] X. Ji, *Phys. Rev. Lett.* **78**, 610 (1997).
- [64] R.L. Jaffe, A. Manohar, *Nucl. Phys.* **B337**, 509 (1990).
- [65] R.L. Jaffe, arXiv:hep-ph/0102281.
- [66] A.V. Belitsky, D. Müller, arXiv:hep-ph/0111037.
- [67] E.R. Berger *et al.*, arXiv:hep-ph/0106192.
- [68] Hermes Collaboration, A. Airapetian *et al.*, *Phys. Rev. Lett.* **87**, 182001 (2001).
- [69] CLAS Collaboration, S. Stepanyan *et al.*, *Phys. Rev. Lett.* **87**, 182002 (2001).
- [70] F. Ellinghaus for the Hermes Collaboration, arXiv:hep-ex/0207029.
- [71] ZEUS Collaboration, S. Chekanov *et al.*, ICHEP02 Abstract 825;  
H1 Collaboration, C. Adloff *et al.*, ICHEP02 Abstract 995;  
<http://www.ichep02.nl/HTMLPages/Sessions/InclSessionList6.shtml>.
- [72] L.L. Frankfurt *et al.*, *Phys. Rev. Lett.* **84**, 2589 (2000).

- [73] H. Avakian for the Hermes Collaboration, see in [89].
- [74] Hermes Collaboration, A. Airapetian *et al.*, *Phys. Lett.* **B535**, 85 (2002).
- [75] J.P. Ralston, D.E. Soper, *Nucl. Phys.* **B152**, 109 (1979).
- [76] V. Barone, A. Drago, P.G. Ratcliffe, arXiv:hep-ph/0104283.
- [77] L. Gamberg, G.R. Goldstein, arXiv:hep-ph/0107176.
- [78] Hermes Collaboration, A. Airapetian *et al.*, *Phys. Rev. Lett.* **84**, 4047 (2000).
- [79] Hermes Collaboration, A. Airapetian *et al.*, *Phys. Rev.* **D64**, 097101 (2001)
- [80] N.C.R. Makins for the Hermes Collaboration, to appear in Proceedings of European Workshop on the QCD Structure of the Nucleon (QCDN02), Castello di Ferrara, Italy, April 3–6, 2002.
- [81] M. Anselmino, arXiv:hep-ph/0107093.
- [82] L. Bland, arXiv:hep-ex/9907058, see also in [88].
- [83] W.-D. Nowak, arXiv:hep-ph/0111218.
- [84] E161 Collaboration, *Measurement of the Polarized Gluon Distribution Using Open Charm Production*, <http://www.slac.stanford.edu/exp/e161>.
- [85] D. Ryckbosch, to appear in [90].
- [86] Proceedings of the 2nd Workshop on Physics with a Polarized-Electron Light-Ion Collider, September, 2000, MIT Cambridge, MA USA, Melville, New York, 2001, AIP conference proceedings Vol. 588.
- [87] Proceedings of the 14th International Spin Physics Symposium (SPIN2000), October 2000, Osaka, Japan, Melville, New York, 2001, AIP conference proceedings Vol. 570.
- [88] Proceedings of the Topical Workshop on Transverse Spin Physics, July 2001, Zeuthen Germany, <http://www-zeuthen.desy.de/spin01>.
- [89] Proceedings of the 8th International Workshop on Deep-Inelastic Scattering, April 2000, Liverpool UK, World Scientific 2000.
- [90] Proceedings of the 9th International Workshop on Deep Inelastic Scattering, April 2001, Bologna Italy, 2001.